Ecological Indicators 125 (2021) 107497

Contents lists available at ScienceDirect

Ecological Indicators

journal homepage: www.elsevier.com/locate/ecolind

Soil phosphorus fractions and distributions in estuarine wetlands with different climax vegetation covers in the Yellow River Delta

Fanzhu Qu [a,b], Ling Meng [a,b,c,*], Jiangbao Xia [a], Haosheng Huang [b,*], Chao Zhan [b], Yunzhao Li [b]

[a] Shandong Key Laboratory of Eco-Environmental Science for the Yellow River Delta, Binzhou University, Binzhou, Shandong 256600, PR China
[b] Department of Oceanography & Coastal Sciences, School of the Coast & Environment, Louisiana State University, Baton Rouge, LA 70803, USA
[c] CAS Key Laboratory of Coastal Environmental Processes and Ecological Remediation, Yantai Institute of Coastal Zone Research, Chinese Academy of Sciences, Yantai Shandong 264003, PR China

ARTICLE INFO

Keywords:
P fractions
Distribution
Climax vegetation cover
Estuarine wetlands
Yellow River Delta

ABSTRACT

To evaluate the relationship between phosphorus (P) fractions and physicochemical characteristics in soils of estuarine wetlands with different climax vegetation covers, surface 60-cm soil samples were collected in *Suaeda heteroptera* wetlands (SH), *Tamarix chinensis* wetlands (TC) and *Phragmites australis* wetlands (PA) in the Yellow River Delta during June 2017. Results showed that the inorganic phosphorus (P_i) in PA soils was significantly lower than that in TC and SH soils ($p < 0.05$), and the organic phosphorus (P_o) showed the opposite pattern, with a rank of PA ≫ TC > SH. The available phosphorus (AP) had a high proportion at surface layer and decreased with increasing depth, with a rank of SH > TC > PA. D.HCl-P_i was the main component of the extracted P_i in all soil profiles, while C.HCl-P_o, NaOH-P_o and Bicarb-P_o were the main components of the extracted P_o in PA, TC and SH soils, respectively. Most of the P_i fractions were significantly positively correlated with Ca, Al and Fe in TC soils, whose correlations were better than those of SH and PA soils, and the P_i fractions were negatively correlated with the pH and sand contents. Our findings confirmed the complexity of the combination and unavailability of P fractions extracted by strong acids. Decreasing of sum of P_o fractions (from14.72% in PA to 11.28% in SH) across a soil salinity gradient (1.0‰ to 12.0‰) provided valuable evidence of the mineralization of soil P_o and that *P. australis* can enhance the biological functions of P. Although difference test revealed clear differences in soil physicochemical properties and slightly clear differences in P fractions, we did not extrapolate real correlations between soil P fractions and climax vegetation covers in this study. Research on the biological mechanism of climax vegetation covers and its influences on the plant absorption and utilization of P is our future direction.

1. Introduction

Phosphorus (P), which occurs as phosphorylated compounds such as adenosine triphosphate and creatine phosphate, for the storage and transmission of energy, and nucleotides (building blocks of DNA and RNA) for the transfer of genetic information, is required for every cell of the living organisms in all biological systems (Dobrota, 2004; Schulze-Makuch and Irwin, 2018). P, as a limiting nutrient in soil for plant growth, is not only an essential factor for eutrophication in the water bodies of natural ecosystems, but also a limiting nutrient in estuaries in China (Koh, 2019; Li et al., 2018; Wu et al., 2019). Rivers are the connections between P sources on land and the ocean, and estuarine wetland processing is an important aspect of P transport from land to the ocean (Bitschofsky and Nausch, 2019). P exists in sediments that erode from upland sources and upstream water, and which have enormous impacts on P physicochemical, biological and biochemical characteristics and processes such as migration, precipitation, dissolution, sorption, desorption, mineralization and immobilization in the P biogeochemical cycle accordingly (Bai et al., 2020). Forms, distribution and availability of P in soils, which are the basis of the estuarine wetland ecosystem, can directly reflect the productivity and functions of coastal wetland ecosystems and the eutrophication risks of coastal and offshore areas (Cui et al., 2018).

In estuarine sediments, P exists in many complex chemical forms with different availabilities that can transform into each other (Gao et al., 2016; Jalali and Matin, 2013; Klamt et al., 2017). An extensive soil

* Corresponding authors at: Binzhou University, 391 Huanghe 5th Rd., Bincheng District, Binzhou 256600, PR China (L. Meng).
E-mail addresses: lmeng@yic.ac.cn (L. Meng), hhuang7@lsu.edu (H. Huang).

https://doi.org/10.1016/j.ecolind.2021.107497
Received 28 December 2020; Received in revised form 1 February 2021; Accepted 3 February 2021
Available online 15 February 2021

P fractionation was presented by Hedley et al. (1982), who partitioned P into inorganic P (P_i), organic P (P_o) and microbial P (P_m) according to their lability in light of availability for plant uptake (Bitschofsky and Nausch, 2019; Qu et al., 2018; Wang et al., 2008). The fractionation has also been improved by Tiessen and Moir (2008) based on many previous approaches. Soil P can be differentiated into the plant-available forms (Resin-P_i, Bicarb-P_i, and Bicarb-P_o) and refractory forms (NaOH-P_i, NaOH-P_o, Dilute HCl-P_i (D.HCl-P_i), Concentrated HCl-P_i (C.HCl-P_i), Concentrated HCl-P_o (C.HCl-P_o) and Residual-P), which are based on the action of anions in acidic or alkaline extractants (Tiessen and Moir, 2008). Resin-P_i is freely exchangeable P_i that can easily dissolve in the soil solution, meanwhile, to some extent, Bicarb-P_i represents P_i which participates in soil respiration. Bicarb-P_i and NaOH-P_i represent a continuum of Fe-P and Al-P. D.HCl-P_i is clearly defined as Ca-P, since Fe-P or Al-P that might remain unextracted after the NaOH extraction is insoluble in acid. C.HCl-P_i and C.HCl-P_o represent stable P forms in residual pools, while Residual-P is the most highly recalcitrant P_i. This fractionation for investigating the availability of P and its transformation can offer a useful index for the relative importance of biological processes to soil P content at different stages of development (Cross and Schlesinger, 1995). However, few studies on sequentially extractable P fractions are available in estuarine wetlands with different climax vegetation covers, especially coupled with the effects of water and salinity gradients in the estuarine region of the Yellow River Delta (YRD), China.

The Yellow River, which played an important role in ancient Chinese civilization, is also called the Huanghe River, and carries 1.08×10^9 t of fluvial sediment annually to the Bohai Sea (Milliman and Meade, 1983; Ye et al., 2006). The YRD is described as the coastal zone with the most active land–ocean interaction in the world (Milliman and Meade, 1983; Yu et al., 2011). However, the land-building rate of new wetlands in the YRD is decreasing with a decrease in the availability of water and sediment in the Yellow River watershed (Liu et al., 2020; Yu et al., 2011; Zhang et al., 2018). To reduce the risk of degradation in coastal estuarine ecosystems of the YRD, flow-sediment regulation via the Xiaolangdi Reservoir has been implemented annually since 2002 (Bai et al., 2020; Gao et al., 2016). In recent years, many studies have focused on the spatiotemporal changes in P fractions in coastal estuarine wetlands of the YRD (Bai et al., 2020; Qu et al., 2018; Yu et al., 2014). However, few studies have focused on the geochemical versus biological processes of soil phosphorus availability and its variations with vegetation cover and hydrologic disturbance in the coastal areas (Wang et al., 2013).

Related studies have found that plants are able to absorb and utilize P in different forms, modify the distribution of soil P among the P pools, and constantly input organic residues to the soil surface, affecting soil P cycling (Davis, 1994; Grunwald et al., 2006; Qu et al., 2018; Sundareshwar and Morris, 1999; Xavier et al., 2010). We hypothesized that 1) the loess deposits are homogeneous within the YRD estuary, and 2) climax vegetation can enhance some of the biogeochemical processes of soil P. Hence, our objectives of this study were (a) to investigate spatial differences in the distributions of soil P fractions under three climax vegetation covers, (b) to reveal the relationships between the content of soil P fractions and basic properties of estuarine wetland soils, and (c) to evaluate the influence of climax vegetation communities on the P availability or P supply power of soil in the YRD estuary.

2. Materials and methods

2.1. Study area description

The studied estuarine wetland region (Fig. 1) is located on the north side of the Yellow River in the YRD National Natural Reserves, which was established to protect newly formed coastal wetlands, and rare and endangered birds, their important habitats, and their breeding or

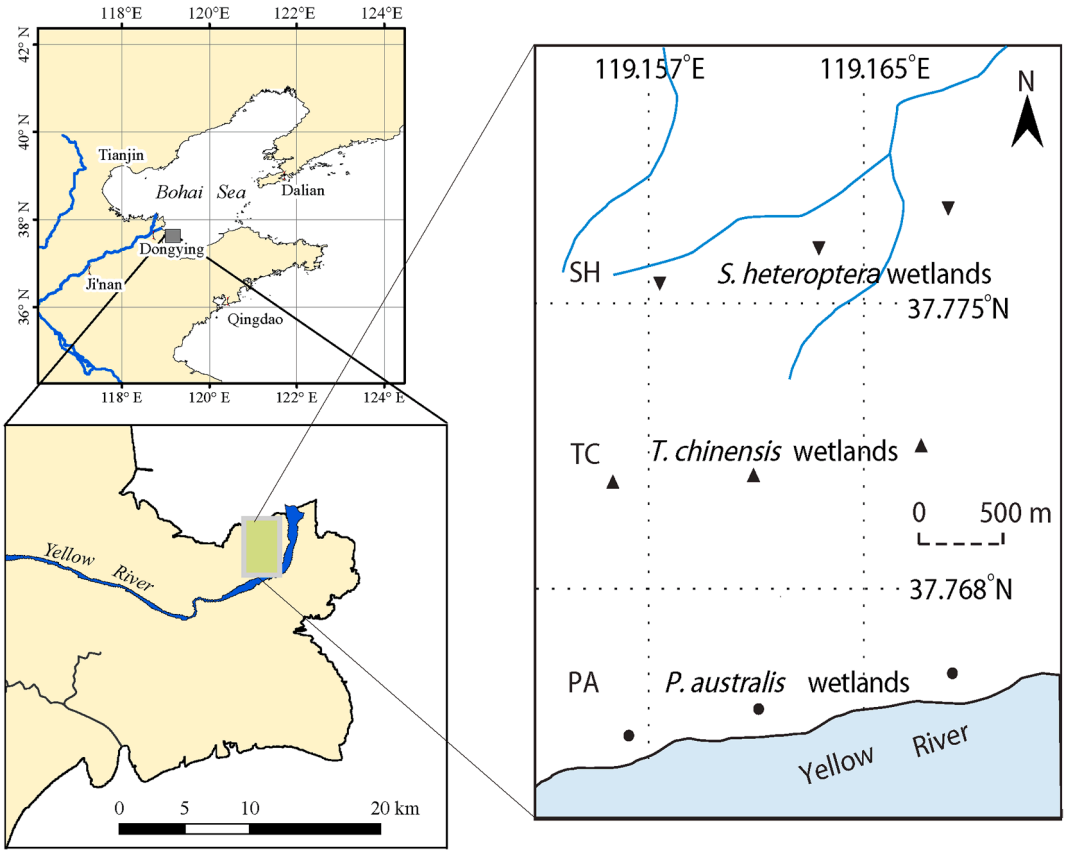

Fig. 1. Sampling plots in estuarine wetlands in the YRD (including: *P. australis* wetlands (PA), *T. chinensis* wetlands (TC) and *S. heteroptera* wetlands (SH)).

stopover places (Ma et al., 2019). Since it was established as a wetland reserve, its extensive and integrated coastal wetland ecosystem is well protected in the warm temperate zone of China. This region, which has four distinct seasons (long hot summers and cold winters, and short windy springs and autumns), is classified as having a warm temperate continental monsoon climate. It has adequate illumination, and its average annual sunshine time is between 2590 h and 2830 h. Its climate is mild, and its frost-free period lasts for approximately 196 d yr^{-1}, with an average annual temperature between 11.7 °C and 12.8 °C. Its natural rainfall is moderate, approximately 530–630 mm yr^{-1}, with uneven seasonal distribution (nearly 70% of the precipitation falls in the summer). Its typical soil type is classified as saline alluvial soil (Fluvisols, FAO) (Meng et al., 2021), and hydrological connectivity is one of the driving factors of plant community distributions and structures in coastal wetlands in the YRD (Dai et al., 2020; Liu et al., 2020). The natural vegetations are cosmopolitan aquatic plants or salt-tolerant plants, such as *Suaeda heteroptera* Kitag., *Tamarix chinensis* Lour., *Imperata cylindrica* (Linn.) Beauv., *Calamagrostis pseudophragmites* (Hall. F.) Koel., *Phragmites australis* (Cav.) Trin. ex Steud., and so on. *S. heteroptera*, *T. chinensis*, and *P. australis* are the three predominant climax vegetation types that mark different vegetation succession phases of the estuarine wetlands in the study area.

2.2. Soil collection and laboratory analyses

To examine the relationship between fractions and distributions of P and physicochemical characteristics of the soils in estuarine wetlands with different climax vegetation covers in the YRD estuary, three kinds of soil sampling plots, i.e., *P. australis* estuarine wetlands (PA), with *P. australis* as the dominant species cover (coverage ≥ 90%) in the surface community; *T. chinensis* estuarine wetlands (TC), with *T. chinensis* as the dominant species cover (coverage ≥ 60%) in the surface community; and *S. heteroptera* estuarine wetlands (SH), with *S. heteroptera* as the dominant species cover (coverage ≥ 99%) in the surface community, were collected during June 25–27, 2017. Five replicates of soil cores with a 60 cm depth were collected in each plot and soil samples were mixed at the same 10 cm interval within a plot. Three plots were collected for each type of estuarine wetland. A total of 45 soil cores were drilled by using a stainless-steel slide hammer, and 54 soil samples were obtained after mixing work. We state that we obtained scientific research permits for the soil collection activity, and confirm that it did not involve or influence endangered or protected species.

Soil samples were stored in Ziploc polyethylene plastic bags immediately after collection. Air-dried soil samples were ground using a mortar and pestle, and then sieved using 0.850 mm and 0.149 mm sieves for laboratory analysis. The P fractions were determined using the modified Hedley sequential fractionation scheme as described in great detail by Tiessen and Moir (2008). The pH value of the 1:5 soil: water suspension was measured with a Beckman pH meter after shaking for 30 min, and electrical conductivity (EC) and salinity were quantified with a conductivity bridge method. Soil organic carbon (SOC) was determined by the dichromate oxidation method. Ca, Al, and Fe in soil samples digested in a $HClO_4$-HNO_3-HF mixture were measured by inductively coupled plasma atomic absorption spectrometry (ICP-AAS-7500 of Shimadzu, Japan). The grain size (sand, silt, and clay) of the soil textural composition was measured by a laser particle analyzer (Malvern Instruments Ltd, Malvern, UK). The chemical analyses were performed at the Shandong Key Laboratory of Eco-Environmental Science for the Yellow River Delta, Binzhou University (BZU).

2.3. Data processing and mapping

A one-way ANOVA (with the Duncan multiple-range test, significant if p is at the 0.05 level) to identify the differences in P fractions and physicochemical characteristics of the soils among estuarine wetlands and a Pearson correlation analysis (significant if p at 0.05 & 0.01 levels) to identify the relationships between P fractions and common physicochemical characteristics with different climax vegetation cover were conducted by using SPSS 18.0. Figures were drawn by using OriginPro 9.1 software packages.

3. Results

3.1. Contents and distributions of P fractions

The mean content and its percentage of P fractions in estuarine wetland soil profiles with different climax vegetation covers in the YRD are shown in Tables S1 and S2. Results showed that the total P (P_t) varied from 649.1 to 705.8 mg kg^{-1}. D.HCl-P_i and Residual-P were the top two fractions of the extracted P_i in all soil profiles, and D.HCl-P_i was the main component of the extracted P_i, which accounted for 58.19–63.94% of the PA, 59.43–67.25% of the TC, and 59.86–63.73% of the SH of the P_t in the soil profiles, respectively. Meanwhile, C.HCl-P_o was the main component of the extracted P_o (6.61–8.06%) in PA, NaOH-P_o (4.63–5.12%) in TC, and Bicarb-P_o (4.48–5.28%) in SH. The vertical distributions of P fractions in estuarine wetland soils with different climax vegetation covers in the YRD estuary are shown in Fig. 2. The lowest point of P_t content appeared in the 30–40 cm layer of PA, 20–30 cm layer of TC, 40–50 cm layer of SH, respectively (Fig. 2, Table S1). The P_t content changed but did not show any obvious regular patterns with depth. D.HCl-P_i showed a similar vertical pattern in all the profiles with different vegetation covers, their lowest contents appeared at the tops of the soils and increased with increasing depth. On the contrary, the total content of plant-available P (AP), which was the sum of Resin-P_i and Bicarb-P_i/P_o accounted for 4.0–6.0% in PA, 4.7–8.2% in TC, and 7.2–8.7% in SH of P_t (Table S2), their highest values occurred at the surface layers and decreased with increasing depth (Figs. 2 and 3). Meanwhile, the minimum value of the mean content of soil P_i occurred in 0–10 cm layer of PA, 10–20 cm layer of TC and 20–30 cm layer of SH (Fig. 3, Table S2). The minimum value of the mean content of soil P_o occurred in the 10–20 cm layer of PA, 20–30 cm layer of TC and 0–10c m layer of SH (Fig. 3, Table S2). No significant trends in the vertical variation of P_i and P_o were present in the soil profiles with different climax vegetation covers (Figs. 2 and 3).

3.2. Differences of soil P fractions

As shown in Table 1, the mean contents of P fractions occurred in the following order: PA (D.HCl-P_i > Residual-P > C.HCl-P_o > C.HCl-P_i > NaOH-P_o > Bicarb-P_o > Resin-P_i > Bicarb-P_i > NaOH-P_o), TC (D.HCl-P_i > Residual-P > C.HCl-P_i > NaOH-P_o > Bicarb-P_o > C.HCl-P_i > Resin-P_i > NaOH-P_o > Bicarb-P_i), and SH (D.HCl-P_i > Residual-P > C.HCl-P_i > Bicarb-P_o > C.HCl-P_o > NaOH-P_o > Resin-P_i > Bicarb-P_i > NaOH-P_i). There was no significant difference in the mean content of soil D.HCl-P_i in estuarine wetland soils with different climax vegetation covers; there was significant difference of Residual-P in PA and SH, no significant difference of Residual-P between PA and TC, between TC and SH (Table 1). There were significant differences in the mean contents of Resin-P_i and Bicarb-P_i and no significant differences in the Bicarb-P_o content in estuarine wetlands with different climax vegetation covers in the YRD. Meanwhile, there were significant differences in the mean contents of AP in soil with different climax vegetation covers, ranked as 53.9 mg kg^{-1} in SH ≫ 47.6 mg kg^{-1} in TC ≫ 36.3 mg kg^{-1} in PA. The Duncan multiple-range test indicated a marked difference in NaOH-P_i between SH (5.9 mg kg^{-1}) and PA (3.6 mg kg^{-1}) and between TC (6.1 mg kg^{-1}) and PA, while the differences between TC and SH were not significant (Table 1). There was a marked difference in NaOH-P_o between TC (33.1 mg kg^{-1}) and SH (22.4 mg kg^{-1}), but no significant differences between TC and PA (25.6 mg kg^{-1}), and between PA and SH (Table 1). It was found that SH had a high mean content of C.HCl-P_i (70.3 mg kg^{-1}) and PA had a high mean content of C.HCl-P_o (49.2 mg kg^{-1}). Meanwhile, there was no significant difference in the mean

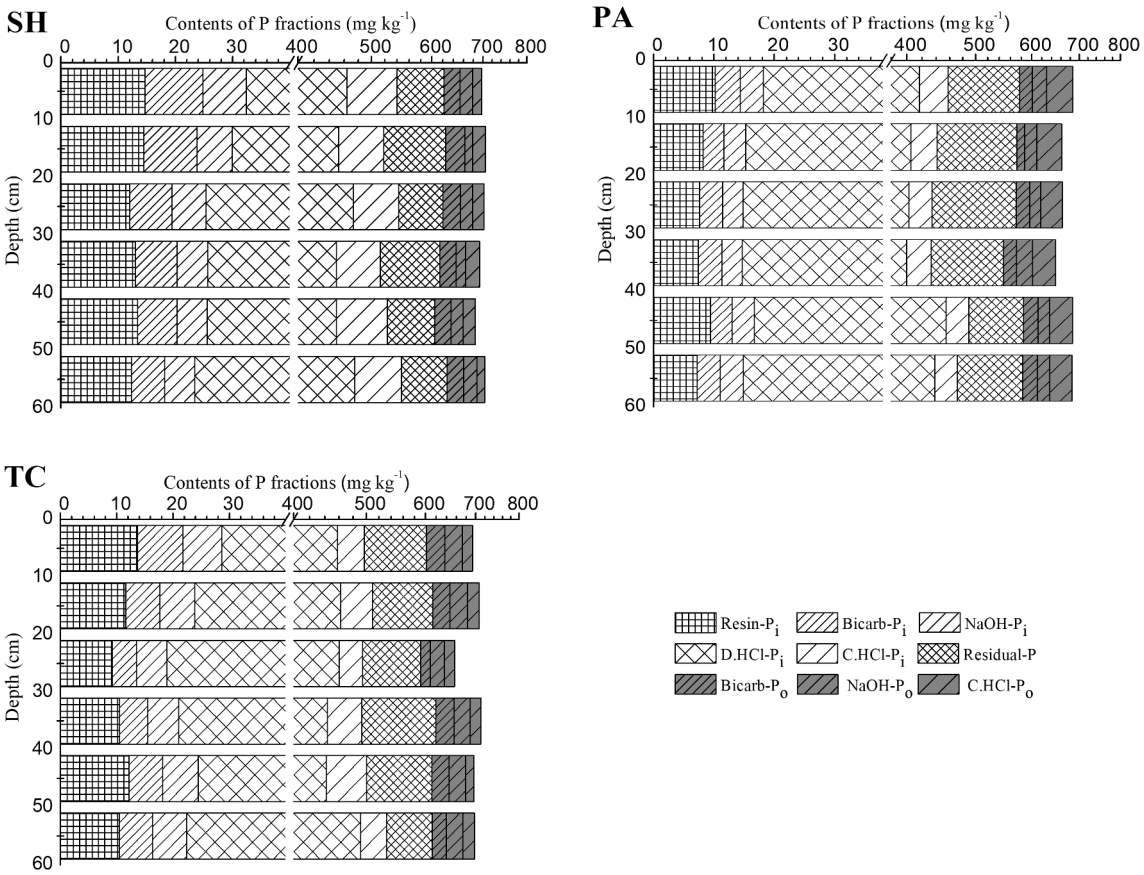

Fig. 2. Vertical distributions of P fractions in the soil profiles of PA, TC and SH.

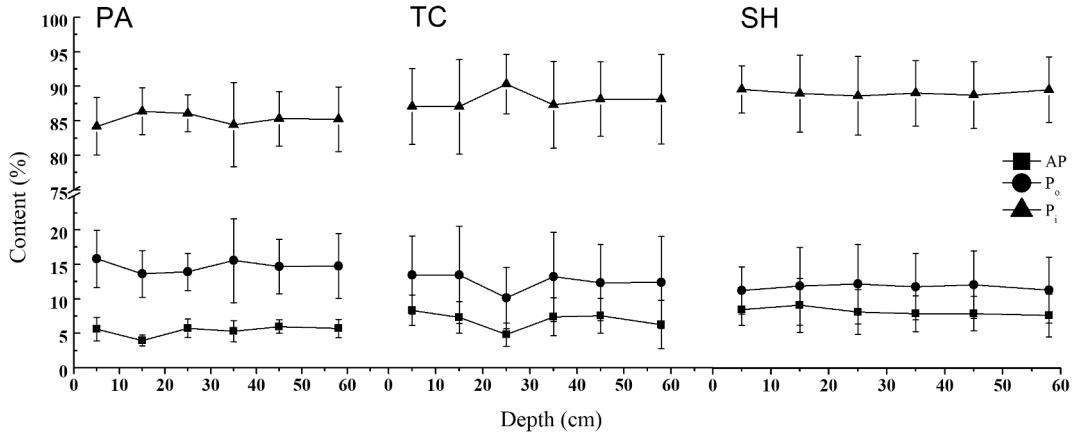

Fig. 3. Change in the percentage of soil P fractions in the PA, TC and SH soil profiles.

content of soil C.HCl-P_i in TC (44.8 mg kg^{-1}) and PA (34.6 mg kg^{-1}) and in the mean content of soil C.HCl-P_o in TC (21.9 mg kg^{-1})and SH (23.5 mg kg^{-1}) (Table 1). Furthermore, there were no significant differences in the mean content of soil P_t of estuarine wetlands with different climax vegetation covers, while the mean contents of P_o were ranked as 98.9 mg kg^{-1} in PA ≫ 85.4 mg kg^{-1} in TC and 78.7 mg kg^{-1} in SH in the YRD (Table 1) and the mean content of P_i was ranked as 530.7 mg kg^{-1} in SH and 504.5 mg kg^{-1} in TC ≫ 454.3 mg kg^{-1} in PA in the YRD (Table 1).

3.3. Physicochemical characteristics

Common physicochemical characteristics of estuarine wetland soils with different climax vegetation covers are listed in Table 2. On the basis of the topography and geomorphology caused by the sedimentation and erosion processes of the Yellow River and Bohai Sea in the estuary, the soils in estuarine wetlands with different climax vegetation covers were classified as solonetz, with high pH values (ranging from 8.5 to 9.1) (Table S3). The mean value of the EC in PA ranged from 282.7 to 476.3 μs/cm, and the mean value of the soil salinity ranged at 0.8–1.2‰; the PA profile was near the river bank and had lower values than that of TC (EC: 2725.1–3323.2 μs/cm; salinity: 6.5–7.9‰) and SH (EC: 3894.5–9291.0 μs/cm, salinity: 9.3–22.0‰), which were on the tidal flat. The soils in PA, TC, and SH were classified into the slightly, moderately and heavily saline-alkaline soil according to soil salinity. The mean content of SOC in PA was 0.4%, TC 0.9%, and SH 0.9%, and the mean content of Fe of PA was 2.6%, TC 3.3% and SH 3.6% (Table 2).

Table 1
Mean content of soil P fractions (listed as mg kg^{-1}) in estuarine wetlands in the YRD.

P fractions	SH	TC	PA
Resin-P_i	13.3 ± 1.9 [a]	11.3 ± 2.6 [b]	8.4 ± 1.5 [c]
Bicarb-P_i	7.8 ± 2.8 [a]	5.9 ± 1.8 [b]	3.8 ± 0.7 [c]
Bicarb-P_o	32.8 ± 14.6 [a]	30.4 ± 15.8 [a]	24.1 ± 9.5 [a]
NaOH-P_i	5.9 ± 1.4 [a]	6.1 ± 1.1 [a]	3.6 ± 0.6 [b]
NaOH-P_o	22.4 ± 11.4[b]	33.1 ± 14.6 [a]	25.6 ± 8.3 [ab]
D.HCl-P_i	433.4 ± 47.2 [a]	436.5 ± 61.0 [a]	403.9 ± 27.2 [a]
C.HCl-P_i	70.3 ± 24.6 [a]	44.8 ± 22.3[b]	34.6 ± 17.7 [b]
C.HCl-P_o	23.5 ± 12.4[b]	21.9 ± 10.2[b]	49.2 ± 20.6 [a]
Residual-P	88.4 ± 19.8[b]	103.8 ± 31.8 [ab]	118.1 ± 29.6 [a]
P_i	530.7 ± 30.5 [a]	504.5 ± 54.9 [a]	454.3 ± 33.0[b]
P_o	78.7 ± 29.4[b]	85.4 ± 35.4[b]	98.9 ± 28.4 [a]
P_t	697.7 ± 21.0 [a]	693.8 ± 50.7 [a]	671.3 ± 39.0 [a]

The superscript a, b and c refer to significant differences between groups, while groups in homogeneous subsets are marked as the superscript ab and bc ($p = 0.05$, $n = 18$).

Table 2
Physicochemical characteristics of soils in estuarine wetlands in the YRD ($p = 0.05$, $n = 18$).

	SH	TC	PA
pH	8.7 ± 0.1 [b]	8.6 ± 0.1 [c]	9.0 ± 0.1 [a]
EC (μs/cm)	5047.8 ± 2061.9 [a]	3131.8 ± 1196.9 [b]	377.8 ± 288.6 [c]
Salinity (‰)	12.0 ± 4.9 [a]	7.5 ± 2.8 [b]	1.0 ± 0.68 [c]
SOC (%)	0.9 ± 0.2 [a]	0.9 ± 0.4 [a]	0.4 ± 0.2 [b]
Ca (%)	5.7 ± 0.6 [a]	5.2 ± 1.0 [b]	4.2 ± 0.4 [c]
Al (%)	7.3 ± 0.6 [a]	6.8 ± 0.6 [b]	6.1 ± 0.3 [c]
Fe (%)	3.6 ± 0.7 [a]	3.3 ± 0.6 [a]	2.6 ± 0.3 [b]
Sand (%)	8.2 ± 5.4 [b]	13.4 ± 9.2 [b]	24.7 ± 11.4 [a]
Silt (%)	76.43 ± 3.4 [a]	77.0 ± 5.9 [a]	70.8 ± 9.5 [b]
Clay (%)	15.4 ± 5.6 [a]	9.6 ± 6.1 [b]	4.5 ± 2.6 [c]

There were no significant differences in the mean contents of SOC and Fe in TC and SH, but significant differences in TC and PA, SH and PA (Table 2). Meanwhile, the mean values of Ca and Fe concentrations in soils under different climax vegetation covers demonstrated obvious variations. There were significant differences in the mean contents of Ca and Al, ranked as SH (Ca 5.7%, Al 7.3%) ≫TC (Ca 5.2%, Al 6.8%) ≫ PA (Ca 4.2%, Al 6.1%) (Table S3). The relative amounts of sand, silt, and clay in estuarine wetland soils with different climax vegetation covers indicated that they were categorized into silt loam with different groundwater conditions. Although, the PA soil contained more sand particles (24.7%) than TC (13.4%) and SH (8.2%) soils, and the SH soil contained more clay particles (15.3%) than TC (9.6%) and PA (4.5%) soils, the silt particles were the major components of soil in PA, TC and SH soils (Tables 2 and S3).

3.4. Relationships between soil P fractions and physicochemical characteristics

The concentrations of soil P fractions can be influenced by the physicochemical characteristics of the soil. Therefore, Pearson correlations of P fractions with common physicochemical characteristics in the study area were investigated, and coefficients are listed in Table 3. The Resin-P_i as well as Bicarb- P_i showed significant positive correlations with Ca ($r = 0.817$, $p < 0.01$; $r = 0.798$, $p < 0.01$) and Al ($r = 0.808$, $p < 0.01$; $r = 0.800$, $p < 0.01$) in soils under three climax vegetation covers. The concentrations of Resin-P_i and Bicarb-P_i showed negative correlations with the pH value ($r = -0.508$, $p < 0.01$; $r = -0.564$, $p < 0.01$) and the percentage of sand ($r = -0.475$, $p < 0.01$; $r = -0.503$, $p < 0.01$), respectively. The NaOH-P_i showed positive correlations with Ca ($r = 0.332$, $p < 0.05$) and Fe ($r = 0.324$, $p < 0.05$), and negative correlations with clay, which was 0.316 ($p < 0.05$). The Pearson correlation analysis results showed that the D.HCl-P_i had significant positive correlations with SOC ($r = 0.697$, $p < 0.01$), Ca ($r = 0.700$, $p < 0.01$) and Fe ($r = 0.495$, $p < 0.01$), but negatively correlated with pH ($r = -0.686$, $p < 0.01$) and sand ($r = -0.503$, $p < 0.01$). Additionally, the P_i was positively correlated with salinity ($r = 0.605$, $p < 0.01$), Ca ($r = 0.450$, $p < 0.01$) and sand ($r = 0.298$, $p < 0.05$), respectively; and negatively correlated with pH ($r = -0.283$, $p < 0.05$) and sand ($r = -0.327$, $p < 0.05$). P_i fractions such as Resin-P_i, Bicarb-P_i and NaOH-P_i showed better correlations with Ca, Al and Fe ions in TC ($p < 0.01$) than which were in PA and SH ($p < 0.05$), and there were no correlations among D.HCl-P_i, C.HCl-P_i, Residual-P_i and physicochemical characteristics ($p > 0.05$) in PA. D.HCl-P_i showed a better negative correlation with Ca and Al ions in SH than which were in PA and TC ($p < 0.01$). Altogether, P_t showed a better positive correlation with salinity ($r = -0.375$, $p < 0.01$) and Ca ($r = 0.400$, $p < 0.01$) in all wetland soils that were investigated.

4. Discussion

4.1. P fractions and physicochemical characteristics of soil in estuarine wetlands

According to the Cowardin classification system (Cowardin et al., 1979), estuarine wetlands are tidal wetlands that are usually semi-enclosed by land and also exposed to a mixture of fresh and brackish water bodies where one or more rivers or streams flow into the ocean. As an ecotone, estuarine wetlands are subject to land and ocean interactions between riverine influences such as flows of freshwater and sediment and marine influences such as tides, waves, and the influx of salt water (Kaiser et al., 2011). Salinity, freshwater input and sediment load, topography, hydrology, and other physicochemical characteristics vary dramatically in estuarine wetlands; in contrast, they all affect the forms and distributions of soil P. Salinity accounts for significant proportions of the variance in the P sorption index (PSI) data, and pH, carbon content and oxalate–extractable Al and Fe are important predictors of PSI data in coastal wetlands (Bruland and DeMent, 2009). Freshwater input improves the maximum P sorption capacity and reduces the desorption rate, and the initial SOC, pH and the exchangeable Al, Fe and Ca contents are important factors (Bai et al., 2017). Sediment load in which P is predominantly bound to particulate matter (PM) fractions, and various hydrologic parameters can influence the transport of each PM and P fraction (Berretta and Sansalone, 2011).

There were no significant differences in P_t in estuarine wetland soils with different climax vegetation covers, and no vertical trends in the variation of P_i and P_o in the three soil profiles were shown in this study (Table 1, Fig. 2), which is similar to our previous finding in the YRD estuary (Qu et al., 2018). In addition, Yu et al. (2014) reported that plant-available P was mainly concentrated in the topsoil layer and decreased with depth in the tidal river network region. A similar phenomenon was observed in wetlands in this study (Figs. 2 and 3). It is well known that D.HCl-P_i was the predominant P fraction and NaOH-P_o was the predominant fraction of total extracted P_o fractions in newly formed wetland soil profiles in the YRD (Xu et al., 2012; Yu et al., 2014). Our results confirmed that the concentrations of the plant-available fractions (Resin-P_i, Bicarb-P_i, and Bicarb-P_o, sum of 6.65%) were low but a higher availability for plant use did not agree with the findings of Xu et al. (2012). Although P_i fractions in soils are unlikely to be in compounds that are simply mixed only by Ca, Al, Fe, and other ions, many sequential extraction methods have tried to extract labile P_i, Al/Fe-bound P_i, Ca-bound P_i, and occluded P_i forms and to establish a relationship between phosphate and metal cations such as Ca, Al and Fe. Significant positive correlations between P_i fractions and Ca, Al and Fe in the study area are direct evidence that Hedley fractionation is a useful method for understanding the relationships between the chemical and biological properties of the soil. Meanwhile, related research has often taken the sum of P_o fractions, which is biological P as an indicator of soil development (Cross and Schlesinger, 1995). Our results revealed that the sum of P_o fractions was a decreasing proportion of the total P_t (14.72% to

Table 3
Pearson correlation coefficients between P fractions and physicochemical characteristics in estuarine wetland soils in the YRD.

		Pearson correlation							
		Resin-P_i	Bicarb-P_i	NaOH-Pi	D.HCl-P_i	C.HCl-P_i	Residual-P_i	P_i	P_t
SH	pH	−0.490*	−0.547*			−0.509*			
	Salinity		0.548*	0.570*					
	TOC	0.684**	0.626**	0.501*	−0.592**				
	Ca	0.617**	0.770**		−0.742**	0.620**		−0.515*	
	Al	0.542*	0.647**		−0.779**	0.697**		−0.538*	
	Fe								
	Sand		−0.512*		0.720**	−0.717**			
	Silt								
	Clay		0.538*		−0.606**	0.612**			
TC	pH				0.619**			0.701**	
	Salinity	0.575*			0.668**	−0.489*	0.755**	0.577*	0.728**
	TOC	0.603**	0.658**	0.588*					
	Ca	0.696**	0.659**	0.585*					
	Al	0.736**	0.723**	0.552*					
	Fe	0.781**	0.776**	0.519*					
	Sand					−0.479*			
	Silt			0.487*		0.509*			
	Clay								
PA	pH			−0.546*					
	Salinity			0.542*					
	TOC								
	Ca	0.558*	0.632**						
	Al		0.684**	0.518*					
	Fe	0.528*	0.574*						
	Sand								
	Silt								
	Clay								
All	pH	−0.508**	−0.475**		−0.686**	−0.301*		−0.283*	
	Salinity	0.758**						0.605**	0.375**
	TOC				0.697**				
	Ca	0.817**	0.798**	0.332*	0.700**			0.450**	0.400**
	Al	0.808**	0.800**	0.360**					
	Fe			0.324*	0.495**				
	Sand	−0.564**	−0.503**		−0.506**		0.303*	−0.327*	
	Silt								
	Clay			0.316*			−0.271*	0.298*	

** Significant at the 0.01 level (2-tailed). * Significant at the 0.05 level (2-tailed).

11.28%) across a soil salinity gradient of 1.0‰ to 12.0‰ and provided valuable evidence of the mineralization of soil P_o from land to the ocean in the estuarine wetlands in the YRD.

4.2. Climax vegetation cover with soil P fractions

It is well known that the YRD is formed by the sediment load of the Yellow River came from water and soil erosion on the Loess Plateau, which has had a relatively low rate of vegetation and a high rate of environmental frailty in the past. After the implementation of the "Grain for Green" project which was substantial for controlling severe soil erosion, vegetation cover on the Loess Plateau was significantly improved (Zhang et al., 2016). Meanwhile, vegetation cover also plays an important role in pedogenic processes in the YRD, which is a new-built estuarine wetland experienced increasingly severe interaction between river and ocean because of the significant decrease in runoff and sediment load of the Yellow River after 2000. Vegetation cover is an important factor to affect the contents of SOC and soil aggregates, which leaving its biomass to increase the input of SOC and to improve soil physical properties, such as mineralogy of the parent material, soil texture, and leaching rates that regulate P availability (Mishra et al., 2013). Numerous studies have found that the concentrations of P fractions in soils or sediments are influenced by litter and root activities as a result of the biological cycles of vegetation (Qualls and Richardson, 2000; Ruess et al., 2019; Yokoyama et al., 2017; Zhang et al., 2015). Plant species and nutritional status can have important influences in various processes and changes in the bioavailability of soil P_i that occurs in the rhizosphere (Hinsinger, 2001; Pii et al., 2015; Schelfhout et al., 2021). Hallama et al. (2019) found that cover crops could enhance the soil microbial community by providing a legacy of increased mycorrhizal abundance, microbial biomass P and phosphatase activity, and had the potential to tighten nutrient cycling under different conditions, increasing crop P nutrition and yield in ecosystems. In this study area, the specific climax vegetation covers are subject to extreme conditions – low soil nutrients, high soil salinity, high potential evapotranspiration, drastic temperature and tide fluctuations – within the estuarine area in the YRD. Vegetation affects soil properties such as pH, ion composition, and soil organic matter content which can increase soil P bioavailability and enhance the use efficiency of P fertilizers (Bornø et al., 2018).

In this study, the AP concentration was lower in the PA soil, in which climax vegetation cover was *P. australis*, compared with the TC soil (climax vegetation cover was *T. chinensis*) and the SH soil (climax vegetation cover was *S. heteroptera*). These results support the view that soil with *S. heteroptera* cover can improve P availability and increase the freely exchangeable P_i, which is consistent with our previous work (Qu et al., 2018). Meanwhile, the vertical distributions of AP in the soil profiles of PA, TC and SH were highest in the surface soils and decreased with depth which was a key point in understanding how plant root and rhizosphere traits determine phosphorus acquisition (Erel et al., 2017; Gahoonia and Nielsen, 2004; Smith et al., 2011). Our results showed that the P_o concentration was higher in the PA soil than that in the TC and SH soils (Table 1, Fig. 3), further revealing that the soils under *P. australis* had higher P adsorption capacities than those under *T. chinensis* and *S. heteroptera*. Considering that there was no significant

difference in P_t concentration among the soils under the different climax vegetation covers, we also found that the P_i concentration in *P. australis* was lower than that in *T. chinensis* and *S.* which confirmed that the soil sediment under *P. australis* has a lower P mineralization ratio, thereby resulting in a net accumulation of P_o in the soils under *P. australis*. This gives direct evidence to the finding that organic P mineralization is promoted with elevated inundation duration of flooding (Sasikala et al., 2009) and is suppressed by low substrate quality (NOE et al., 2013). Moreover, the clear differences in soil physicochemical properties and P fractions found in PA, TC, and SH which confirmed that vegetation and soil mutually influence each other, and neither is the result of the other, although we were still unable to extrapolate real correlations between soils and climax vegetation covers in the study area.

5. Conclusions

We investigated the soil phosphorus fractions and distributions in estuarine wetland soils with different climax vegetation covers. Our results confirmed that soil P exists in many complex chemical fractions, most of which have no obvious trends in vertical distribution in soil profiles. P_i fractions were significantly correlated with Ca, Al, and Fe and availability of P fractions that were associated with the different soil mineral ions. The predominant fractions of P_o in soils under different climax vegetation covers markedly differed in both contents and distributions. *P. australis* enhanced the biological functions of soil P and soils under *S. heteroptera* had a higher proportion of P_o mineralization. These data revealed that climax vegetation cover dramatically influenced P fractions and distributions in estuarine wetland soils. The influence of different vegetation covers in estuarine wetlands on the availability and conversion of P fractions will be the subject of future research.

CRediT authorship contribution statement

Fanzhu Qu: Writing - original draft, Methodology, Investigation, Data curation, Software, Conceptualization, Funding acquisition. **Ling Meng:** Writing - review & editing, Conceptualization, Project administration. **Jiangbao Xia:** Investigation, Methodology, Project administration, Funding acquisition, Supervision. **Haosheng Huang:** Writing - review & editing, Conceptualization. **Chao Zhan:** Investigation, Methodology, Supervision, Supervision. **Yunzhao Li:** Investigation, Data curation, Methodology, Supervision.

Declaration of Competing Interest

The authors declare that they have no known competing financial interests or personal relationships that could have appeared to influence the work reported in this paper.

Acknowledgments

This study was supported by the National Key R&D Program of China (Grant No. 2017YFC0505904), the National Natural Science Foundation of China (Grant No. 431870468, 1501088), the Taishan Scholars Program of Shandong Province, China (Grant No. TSQN201909152) and Shandong Provincial Natural Science Foundation, China (Grant No. ZR2020QD092). We also would like to thank Shandong Key Laboratory of Eco-Environmental Science for the Yellow River Delta, BZU for the help with experimental analyses for this study.

Appendix A. Supplementary data

Supplementary data to this article can be found online at https://doi.org/10.1016/j.ecolind.2021.107497.

References

Bai, J., Ye, X., Jia, J., Zhang, G., Zhao, Q., Cui, B., Liu, X., 2017. Phosphorus sorption-desorption and effects of temperature, pH and salinity on phosphorus sorption in marsh soils from coastal wetlands with different flooding conditions. Chemosphere 188, 677–688. https://doi.org/10.1016/j.chemosphere.2017.08.117.

Bai, J., Yu, L., Ye, X., Yu, Z., Wang, D., Guan, Y., Cui, B., Liu, X., 2020. Dynamics of phosphorus fractions in surface soils of different flooding wetlands before and after flow-sediment regulation in the Yellow River Estuary, China. J. Hydrol. 580, 124256. https://doi.org/10.1016/j.jhydrol.2019.124256.

Berretta, C., Sansalone, J., 2011. Hydrologic transport and partitioning of phosphorus fractions. J. Hydrol. 403 (1-2), 25–36. https://doi.org/10.1016/j.jhydrol.2011.03.035.

Bitschofsky, F., Nausch, M., 2019. Spatial and seasonal variations in phosphorus speciation along a river in a lowland catchment (Warnow, Germany). Sci. Total Environ. 657, 671–685. https://doi.org/10.1016/j.scitotenv.2018.12.009.

Bornø, M.L., Müller-Stöver, D.S., Liu, F., 2018. Contrasting effects of biochar on phosphorus dynamics and bioavailability in different soil types. Sci. The Total Environ. 627, 963–974. https://doi.org/10.1016/j.scitotenv.2018.01.283.

Bruland, G.L., DeMent, G., 2009. Phosphorus sorption dynamics of Hawaii's Coastal Wetlands. Estuaries Coasts 32 (5), 844–854. https://doi.org/10.1007/s12237-009-9201-9.

Cowardin, L.M., Carter, V., Golet, F.C., LaRoe, E.T., 1979. Classification of Wetlands and Deepwater Habitats of the United States, first ed. Fish and Wildlife Service, US Department of the Interior, Washington, D.C.

Cross, A.F., Schlesinger, W.H., 1995. A literature review and evaluation of the. Hedley fractionation: applications to the biogeochemical cycle of soil phosphorus in natural ecosystems. Geoderma 64 (3-4), 197–214. https://doi.org/10.1016/0016-7061(94)00023-4.

Cui, Y., Xiao, R., Xie, Y., Zhang, M., 2018. Phosphorus fraction and phosphate sorption-release characteristics of the wetland sediments in the Yellow River Delta. Phys. Chem. Earth 2002 (103), 19–27. https://doi.org/10.1016/j.pce.2017.06.005.

Dai, L., Zhang, Y., Liu, Y., Xie, L., Zhao, S., Zhang, Z., Xizhi, L.v., 2020. Assessing hydrological connectivity of wetlands by dye-tracing experiment. Ecol. Indic. 119, 106840. https://doi.org/10.1016/j.ecolind.2020.106840.

Davis, S.M., 1994. Phosphorous inputs and vegetation sensitivity in the everglades. In: Davis, S.M., Ogden, J.C. (Eds.), Everglades: The Ecosystem and Its Restoration, first ed. CRC Press, Boca Raton, Florida, pp. 357–378.

Dobrota, C., 2004. The biology of phosphorus. In: Valsami-Jones, E. (Ed.), Phosphorus in Environmental Technology: Principles and Applications, first ed. IWA publishing, London, pp. 51–78.

Erel, R., Bérard, A., Capowiez, L., Doussan, C., Arnal, D., Souche, G., Gavaland, A., Fritz, C., Visser, E.J.W., Salvi, S., Le Marié, C., Hund, A., Hinsinger, P., 2017. Soil type determines how root and rhizosphere traits relate to phosphorus acquisition in field-grown maize genotypes. Plant Soil 412 (1-2), 115–132. https://doi.org/10.1007/s11104-016-3127-3.

Gahoonia, T.S., Nielsen, N.E., 2004. Root traits as tools for creating phosphorus efficient crop varieties. Plant and Soil 260 (1/2), 47–57. https://doi.org/10.1023/B:PLSO.0000030168.53340.bc.

Gao, Z., Fang, H., Bai, J., Jia, J., Lu, Q., Wang, J., Chen, B., 2016. Spatial and seasonal distributions of soil phosphorus in a short-term flooding wetland of the Yellow River Estuary, China. Ecol. Inf. 31, 83–90. https://doi.org/10.1016/j.ecoinf.2015.10.010.

Grunwald, S., Corstanje, R., Weinrich, B.E., Reddy, K.R., 2006. Spatial patterns of labile forms of phosphorus in a subtropical Wetland. J. Environ. Qual. 35 (1), 378–389. https://doi.org/10.2134/jeq2005.0042.

Hallama, M., Pekrun, C., Lambers, H., Kandeler, E., 2019. Hidden miners – the roles of cover crops and soil microorganisms in phosphorus cycling through agroecosystems. Plant Soil 434, 7–45. https://doi.org/10.1007/s11104-018-3810-7.

Hinsinger, P., 2001. Bioavailability of soil inorganic P in the rhizosphere as affected by root-induced chemical changes: a review. Plant Soil 237 (2), 173–195. https://doi.org/10.1023/A:1013351617532.

Jalali, M., Matin, N.H., 2013. Soil phosphorus forms and their variations in selected paddy soils of Iran. Environ. Monit. Assess. 185 (10), 8557–8565. https://doi.org/10.1007/s10661-013-3195-2.

Kaiser, M.J., Barnes, D.K.A., Jennings, S., Attrill, M., Thomas, D.N., 2011. Marine Ecology: Processes, Systems and Impacts, second ed. Oxford University Press, New York.

Klamt, A.-M., Jensen, H.S., Mortensen, M.F., Schreiber, N., Reitzel, K., 2017. The importance of catchment vegetation for alkalinity, phosphorus burial and macrophytes as revealed by a recent paleolimnological study in a soft water lake. Sci. The Total Environ. 580, 1097–1107. https://doi.org/10.1016/j.scitotenv.2016.12.065.

Koh, H.-S., 2019. Using algal biomass-phosphorus (P) relationships and nutrient limitation theory to evaluate the adequacy of P water quality criteria for regulated monsoon rivers and reservoirs. Chem. Ecol. 35 (5), 408–430. https://doi.org/10.1080/02757540.2019.1567719.

Li, J., Lai, Y., Xie, R., Ding, X., Wu, C., 2018. Sediment phosphorus speciation and retention process affected by invasion time of Spartina alterniflora in a subtropical coastal wetland of China. Environ. Sci. Pollut. Res. 25 (35), 35365–35375. https://doi.org/10.1007/s11356-018-3447-3.

Liu, J., Engel, B.A., Zhang, G., Wang, Y.u., Wu, Y., Zhang, M., Zhang, Z., 2020. Hydrological connectivity: One of the driving factors of plant communities in the Yellow River Delta. Ecol. Indic. 112, 106150. https://doi.org/10.1016/j.ecolind.2020.106150.

Ma, T., Li, X., Bai, J., Ding, S., Zhou, F., Cui, B., 2019. Four decades' dynamics of coastal blue carbon storage driven by land use/land cover transformation under natural and

anthropogenic processes in the Yellow River Delta, China. Sci. The Total Environ. 655, 741–750. https://doi.org/10.1016/j.scitotenv.2018.11.287.
Meng, L., Qu, F., Bi, X., Xia, J., Li, Y., Wang, X., Yu, J., 2021. Elemental stoichiometry (C, N, P) of soil in the Yellow River Delta nature reserve: Understanding N and P status of soil in the coastal estuary. Sci. The Total Environ. 751, 141737. https://doi.org/10.1016/j.scitotenv.2020.141737.
Milliman, J.D., Meade, R.H., 1983. World-wide delivery of river sediment to the oceans. J. Geol. 91 (1), 1–21. https://doi.org/10.1086/628741.
Mishra, A., Tripathi, J.K., Mehta, P., Rajamani, V., 2013. Phosphorus distribution and fractionation during weathering of amphibolites and gneisses in different climatic setups of the Kaveri river catchment, India. Appl. Geochem. 33, 173–181. https://doi.org/10.1016/j.apgeochem.2013.02.010.
Noe, G.B., Hupp, C.R., Rybicki, N.B., 2013. Hydrogeomorphology influences soil nitrogen and phosphorus mineralization in floodplain wetlands. Ecosystems 16 (1), 75–94 https://doi.org/110.1007/s10021-012-9597-0.
Pii, Y., Mimmo, T., Tomasi, N., Terzano, R., Cesco, S., Crecchio, C., 2015. Microbial interactions in the rhizosphere: beneficial influences of plant growth-promoting rhizobacteria on nutrient acquisition process. A review. Biol. Fertil. Soils 51 (4), 403–415. https://doi.org/10.1007/s00374-015-0996-1.
Qu, F., Shao, H., Meng, L., Yu, J., Xia, J., Sun, J., Li, Y., 2018. Forms and vertical distributions of soil phosphorus in newly formed coastal wetlands in the Yellow River Delta estuary. Land Degrad. Dev. 29 (11), 4219–4226. https://doi.org/10.1002/ldr.3132.
Qualls, R.G., Richardson, C.J., 2000. Phosphorus enrichment affects litter decomposition, immobilization, and soil microbial phosphorus in wetland mesocosms. Soil Sci. Soc. Am. J. 64 (2), 799–808. https://doi.org/10.2136/sssaj2000.642799x.
Ruess, R.W., McFarland, J.W., Person, B., Sedinger, J.S., 2019. Geese mediate vegetation state changes with parallel effects on N cycling that leave nutritional legacies for offspring. Ecosphere 10 (8). https://doi.org/10.1002/ecs2.2850.
Sasikala, S., Tanaka, N., Wah, H.S.Y.W., Jinadasa, K.B.S.N., 2009. Effects of water level fluctuation on radial oxygen loss, root porosity, and nitrogen removal in subsurface vertical flow wetland mesocosms. Ecol. Eng. 35 (3), 410–417. https://doi.org/10.1016/j.ecoleng.2008.10.003.
Schelfhout, S., Wasof, S., Mertens, J., Vanhellemont, M., Demey, A., Haegeman, A., DeCock, E., Moeneclaey, I., Vangansbeke, P., Viaene, N., Baeyen, S., De Sutter, N., Maes, M., van der Putten, W.H., Verheyen, K., De Schrijver, A.n., 2021. Effects of bioavailable phosphorus and soil biota on typical Nardus grassland species in competition with fast-growing plant species. Ecol. Indic. 120, 106880. https://doi.org/10.1016/j.ecolind.2020.106880.
Schulze-Makuch, D., Irwin, L.N., 2018. Life in the Universe: Expectations and Constraints, third ed. Springer, Berlin, Germany.
Smith, S.E., Jakobsen, I., Grønlund, M., Smith, F.A., 2011. Roles of arbuscular mycorrhizas in plant phosphorus nutrition: interactions between pathways of phosphorus uptake in arbuscular mycorrhizal roots have important implications for understanding and manipulating plant phosphorus acquisition. Plant. Physiol. 156 (3), 1050–1057. https://doi.org/10.1104/pp.111.174581.
Sundareshwar, P.V., Morris, J.T., 1999. Phosphorus sorption characteristics of intertidal marsh sediments along an estuarine salinity gradient. Limnol. Oceanogr. 44 (7), 1693–1701. https://doi.org/10.4319/lo.1999.44.7.1693.
Tiessen, H., Moir, J.O., 2008. Characterization of available P by sequential extraction. In: Cater, M.R., Gregorich, E.G. (Eds.), Soil Sampling and Methods of Analysis, second ed. CRC Press, Boca Raton, Florida, pp. 293–306.
Wang, G.-P., Zhai, Z.-L., Liu, J.-S., Wang, J.-D., 2008. Forms and profile distribution of soil phosphorus in four wetlands across gradients of sand desertification in Northeast China. Geoderma 145 (1-2), 50–59. https://doi.org/10.1016/j.geoderma.2008.02.004.
Wang, L., Ye, M., Li, Q., Zou, H., Zhou, Y., 2013. Phosphorus speciation in wetland sediments of Zhujiang (Pearl) River Estuary, China. Chin. Geogr. Sci. 23 (5), 574–583. https://doi.org/10.1007/s11769-013-0627-4.
Wu, G., Cao, W., Wang, F., Su, X., Yan, Y., Guan, Q., 2019. Riverine nutrient fluxes and environmental effects on China's estuaries. Sci. The Total Environ. 661, 130–137. https://doi.org/10.1016/j.scitotenv.2019.01.120.
Xavier, F.A.d.S., Almeida, E.F., Cardoso, I.M., de Sá Mendonça, E., 2010. Soil phosphorus distribution in sequentially extracted fractions in tropical coffee-agroecosystems in the Atlantic Forest biome, Southeastern Brazil. Nutr. Cycl. Agroecosyst. 89 (1), 31–44. https://doi.org/10.1007/s10705-010-9373-5.
Xu, G., Shao, H.-B., Sun, J.-N., Chang, S.X., 2012. Phosphorus fractions and profile distribution in newly formed wetland soils along a salinity gradient in the Yellow River Delta in China. Z. Pflanzenernähr. Bodenk. 175 (5), 721–728. https://doi.org/10.1002/jpln.201100307.
Ye, Q., Chen, S., Chen, Q., Huang, C., Tian, G., Chen, S., Shi, Y., Liu, Q., Liu, G., 2006. Spatial-temporal characteristics in landscape evolution of the Yellow River Delta during 1855–2000 and a way out for the Yellow River estuary. Chin. Sci. Bull. 51 (Supp.), 197–209. https://doi.org/10.1007/s11434-006-8197-9.
Yokoyama, D., Imai, N., Kitayama, K., 2017. Effects of nitrogen and phosphorus fertilization on the activities of four different classes of fine-root and soil phosphatases in Bornean tropical rain forests. Plant. Soil 416 (1-2), 463–476. https://doi.org/10.1007/s11104-017-3225-x.
Yu, J., Fu, Y., Li, Y., Han, G., Wang, Y., Zhou, D., Sun, W., Gao, Y., Meixner, F.X., 2011. Effects of water discharge and sediment load on evolution of modern Yellow River Delta, China, over the period from 1976 to 2009. Biogeosciences 8 (9), 2427–2435. https://doi.org/10.5194/bg-8-2427-2011.
Yu, J., Qu, F., Wu, H., Meng, L., Du, S., Xie, B., 2014. Soil phosphorus forms and profile distributions in the tidal river network region in the Yellow River Delta Estuary. Sci. World J. 2014, 1–11. https://doi.org/10.1155/2014/912083.
Zhang, B., He, C., Burnham, M., Zhang, L., 2016. Evaluating the coupling effects of climate aridity and vegetation restoration on soil erosion over the Loess Plateau in China. Sci. Total Environ. 539, 436–449. https://doi.org/10.1016/j.scitotenv.2015.08.132.
Zhang, W., Zeng, C., Tong, C., Zhai, S., Lin, X., Gao, D., 2015. Spatial distribution of phosphorus speciation in marsh sediments along a hydrologic gradient in a subtropical estuarine wetland, China. Estuar. Coast. Shelf Sci. 154 (5), 30–38. https://doi.org/10.1016/j.ecss.2014.12.023.
Zhang, X., Yang, Z., Zhang, Y., Ji, Y., Wang, H., Lv, K., Lu, Z., 2018. Spatial and temporal shoreline changes of the southern Yellow River (Huanghe) Delta in 1976–2016. Mar. Geol. 395, 188–197. https://doi.org/10.1016/j.margeo.2017.10.006.